This article has been accepted for publication in a future issue of this journal, but has not been fully edited. Content may change prior to final publication. Citation information: DOI 10.1109/TAP.2020.2995315, IEEE Transactions on Antennas and Propagation

Near-field Constrained Design for Self-tuning UHF-RFID Antennas

G. M. Bianco, S. Amendola, G. Marrocco

***Abstract*—Recently introduced self-tuning RFID tags are capable to dynamically modify the input impedance of the embedded microchip transponder in order to compensate possible impedance mismatch with the antenna, thus making the communication performance rather insensitive to the nearby environment. A general method for the design of this new class of tags is presented with the purpose to master the complex configuration, where the tag is placed at a close distance from the interrogating antenna and the free-space assumption is not valid. A two-port system is introduced and the network-oriented reformulation of self-tuning action permits to derive an optimization problem for the minimization of the interrogation power for a wide range of boundary conditions. The method is demonstrated, both numerically and experimentally, through the application of a Finger Augmentation Device aimed to achieve a smart interaction with touched objects.**

***Index Terms*—Radiofrequency Identification, self-tuning antennas, electromagnetic coupling, constrained design, Near Field.**

I. Introduction[1]

Recently introduced *self-tuning* RFID tags [1], [2], [3] in the UHF band (860-950 MHz) are capable of dynamically modifying the input impedance of the embedded integrated circuit (IC) transponder, in order to compensate the impedance mismatch with the antenna that occurs when the boundary conditions change. Such devices offer an unprecedented bandwidth and permit to keep the power transfer coefficient of the tag nearly invariant when it is attached on objects made of different materials.

The general theory of self-tuning tags, in both linear and non-linear regimes, was presented in [4] and an application to temperature measurement was explored in [5]. In those works the modeling of the chip assumes the reader and tag to be electromagnetically decoupled, namely being in far-field condition. In some applications, however, the reader has to be placed at a very short distance from the tag, for examples in biomedical systems where tags are implanted inside the body to collect Electromyography (EMG) [6] and Electroencephalogram (EEG) [7] signals, intracranial pressure [8] or they are integrated within prostheses [9] to measure the internal temperature. The electromagnetic coupling also occurs in Radiofrequency Finger-Augmentation-Devices (R-FAD) [10], consisting of sensing antennas attached over the fingertip of human or robotic hands to collect some physical parameter (e.g. temperature) of the touched object and transmit it to a reader module mounted on the wrist. Further possible scenarios include the monitoring of the temperature inside shielding metallic enclosures (e.g. Cyclotron Auto-Resonance Maser [11] or vulcanization mold [12]) and the combined powering and reading of remotely located passive-resistive temperature probes in industrial settings [13]. Finally, near field UHF links systems can involve desktop readers and the emerging paradigm of the *Tactile Internet* [14] where human senses will interact with machines. In all the above applications, the design of the tag antenna connected to a self-tuning chip cannot take benefit from the usual free-space representation, involving standalone impedance and radiation power gain, since the performance of the self-tuning tags has to be instead evaluated by accounting for the proximal presence of the reader.

This paper introduces a general-purpose design methodology of the self-tuning RFID antenna that includes the electromagnetic coupling with the interrogating antenna. The two-fold aim is maximizing the performance of the RFID link and making the communication insensitive to the variability of the surrounding environment. The proposed method is based on the generalization of the self-tuning equations [4] in terms of *embedded* admittance and *transducer power gain* of a two-port network. The design of the tag antenna is hence formulated as constrained optimization to exploit the whole self-tuning range of the chip.

The paper is organized as follows. Section II introduces the coupling model for near-field reader-tag interaction including the dynamic admittance of the IC. Constrained optimization is described in Section III. The method is then applied to the design of an R-FAD device to achieve robust communication performance with regard to the touched object. The numerical procedure is finally validated through experimental measurements on prototypes (Section IV).

II. Electromagnetic model of the coupled RFID link

A. Self-tuning ICs

Self-tuning ICs are a new class of RFID transponder that includes an analog front-end with a voltage-controlled capacitor that is automatically adjusted, depending upon the open-circuit voltage that is induced at the port of the tag antenna, to maximize the power the tag's antenna delivers to the IC itself. Denoting with $Y_{IC} = G_{IC} + j\omega C_{IC}$ the radiofrequency equivalent admittance of the IC, the self-tuning capacitor can be parametrized as

$$C_{IC}(n) = C_{min} + nC_{step} \tag{1}$$

[1]Authors are with the Pervasive Electromagnetics Lab, University of Roma Tor Vergata, www.pervasive.ing.uniroma2.it. Corresponding author: gaetano.marrocco@uniroma2.it

This article has been accepted for publication in a future issue of this journal, but has not been fully edited. Content may change prior to final publication. Citation information: DOI 10.1109/TAP.2020.2995315, IEEE Transactions on Antennas and Propagation

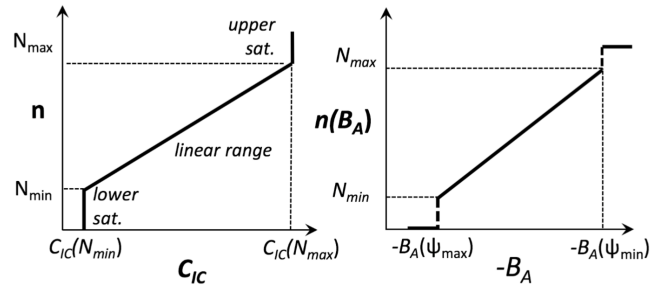

Figure 1. Characteristic curves of Self-tuning ICs: a) relationship between the variable IC capacitance and the tuning parameter *n*, which accounts for the self-tuning quantization; b) mapping of the susceptance $B_A(\psi)$ of the tag with respect to the boundary conditions that are generically parametrized with $\psi_{min} \leq \psi \leq \psi_{max}$ within the linear region of the IC ($N_{min} \leq n \leq N_{max}$), where the parameter *n* accounts for the re-tuning quantization.

where $N_{min} \leq n \leq N_{max}$ and C_{step} account for re-tuning quantization. Being $Y_A = G_A + jB_A$ the admittance of the tag antenna, the capacitance of the IC is automatically adjusted so that

$$|\omega C_{IC}(n) + B_A| \rightarrow 0. \tag{2}$$

For the sake of generality, a saturation effect (Fig.1.a) occurring outside a *linear* range is also included so that

$$C_{IC}(n < N_{min}) = C_{IC}(N_{min}) \tag{3}$$
$$C_{IC}(n > N_{max}) = C_{IC}(N_{max}) \tag{4}$$

Accordingly, the retuning index *n* is related to the antenna admittance as

$$n = nint\left(-\frac{1}{C_{step}}\left(C_{IC}\left(N_{min}\right) + \frac{B_A}{\omega}\right)\right) \tag{5}$$

where "nint" stands for the Nearest Integer function so that nint(x) is the integer number closest to x.

B. Two-port model of coupled RFID link

Let us now consider that the self-tuning tag is placed in close proximity of the interrogating antenna so that the tag input admittance is affected by the presence of the reader itself. With reference to Fig. 2, the Norton equivalent model with Admittance matrix $[Y]$ is exploited to derive the *embedded* input admittance of the tag antenna as well as the *Transducer Power Gain* G_T[2] to parametrize the reader-tag interaction.

By assuming a reciprocal two-port network and by following a dual formulation with respect to [10], wherein the T-equivalent circuit of the network is replaced by a Π-equivalent topology, the input admittance Y_{out} seen from the IC port towards the network is

[2]The Transducer Power Gain is defined as the ratio between the power delivered by the network to the load (here the IC) and the available power from the generator. This parameter is a feature of the whole link and it is therefore more general than the realized gain of an antenna as it also accounts for the mutual interaction among the transmitting and receiving antennas as well as for the effect of the nearby environment.

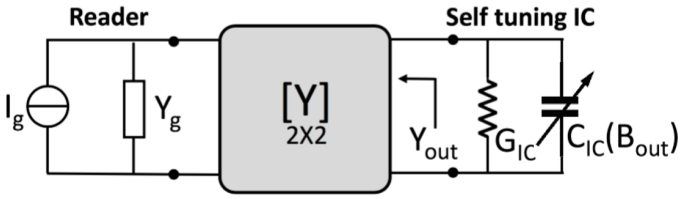

Figure 2. Two-port network model of the RFID link where the self-tuning IC is accounted for by a variable capacitor whose value is a dynamic function of the susceptance B_{out} seen from the IC terminal toward the network.

$$Y_{out} = G_{out} + jB_{out} = Y_{22} - \frac{Y_{12}^2}{Y_{11} + Y_g} \tag{6}$$

being $Y_g = G_g + jB_g$ the internal admittance of the reader. B_{out} is hence the embedded antenna susceptance to be inserted in (2) instead of B_A.

Similarly, by applying the dual formulation than in [10], the Transducer Power Gain can be expressed as:

$$G_T = \frac{4G_g G_{IC}\left|Y_{12}\right|^2}{\left|\left(Y_{11}+Y_g\right)\left(Y_{22}+Y_{IC}\right) - Y_{12}^2\right|^2} \tag{7}$$

Finally, by exploiting the self-tuning behavior of the IC, the transducer power gain can be derived from, (2) and (7) for the linear and saturation regimes of the chip retuning:

$$G_{T=}\begin{cases} \frac{4G_g G_{IC}|Y_{12}|^2}{\left|(Y_{11}+Y_g)(Y_{22}+G_{IC}+j\omega C_{IC}(N_{min}))-Y_{12}^2\right|^2} \\ if\ B_{out} \geq -\omega C_{IC}(N_{min}) \\ \\ \frac{4G_g G_{IC}|Y_{12}|^2}{\left|(Y_{11}+Y_g)(Y_{22}+G_{IC}-jB_{out})-Y_{12}^2\right|^2} \\ if\ -\omega C_{IC}\left(N_{max}\right) < B_{out} < -\omega C_{IC}(N_{min}) \\ \\ \frac{4G_g G_{IC}|Y_{12}|^2}{\left|(Y_{11}+Y_g)(Y_{22}+G_{IC}+j\omega C_{IC}(N_{max}))-Y_{12}^2\right|^2} \\ if\ B_{out} \leq -\omega C_{IC}\left(N_{max}\right) \end{cases} \tag{8}$$

III. Constrained Optimization

A. Problem formulation

Denote with $\psi_{min} < \psi < \psi_{max}$ the physical parameter of the boundary conditions with respect to which the communication performance of the self-tuning tag has to be maximized and kept stable. Such a parameter could be for instance the electric permittivity of the object the tag is touching (as in the next experimental example) but also the frequency at the purpose to broaden the link bandwidth.

To activate the RFID link, the turn-on power P_{to} (i.e. the minimum power the reader has to emit to activate the remote tag) must be lower than the maximum value $P_{av,max}$ that is available by the transmitter, even in the worst-case scenario concerning the parameter ψ. P_{to} is proportional to the power sensitivity (p_{IC}) of the IC through G_T. The communication constraint is, therefore:

This article has been accepted for publication in a future issue of this journal, but has not been fully edited. Content may change prior to final publication. Citation information: DOI 10.1109/TAP.2020.2995315, IEEE Transactions on Antennas and Propagation

$$P_{to}(\psi) = \frac{p_{IC}}{G_T(\psi)} \leq P_{av,max}, \qquad \text{for } \psi_{min} \leq \psi \leq \psi_{max} \tag{9}$$

where $G_T(\psi)$ is derived from (8) by considering the dependence $\{Y_{ij}(\psi)\}$. Moreover, to exploit the full self-tuning capability of the IC, the antenna susceptance $B_A(\psi_{min} \leq \psi \leq \psi_{max})$ has to be exactly mapped within the whole linear region of the self-tuning IC for the possible values of the boundary conditions. With reference to Fig. 1.b and from (5) the following design constraints have to be accordingly matched:

$$n(\psi_{max}) \rightarrow N_{min}, \qquad n(\psi_{min}) \rightarrow N_{max} \tag{10}$$

where, by any loss of generality, we assumed that $B_A(\psi_{max}) > B_A(\psi_{min})$.

B. Penalty function

Let $\bar{\mathbf{a}} = \{a_1, a_2, .., a_M\}$ denote the set of geometrical parameters of the tag antenna to be optimized for matching the above constraints. The optimization problem is formalized as the minimization of the following *penalty function*:

$$U(\bar{\mathbf{a}}) = \sum_{i=1}^{3} w_i u_i(\bar{\mathbf{a}}) \tag{11}$$

where:

$$u_1 = \begin{cases} \left|1 - \frac{|B_A(\psi_{max})[\bar{\mathbf{a}}]|}{\omega C_{IC}(N_{min})}\right| \\ \text{if } C_{IC}(N_{min}) \leq -\frac{B_A(\psi_{max})}{\omega} \leq C_{IC}(N_{max}) \\ 1 \qquad \text{otherwise} \end{cases} \tag{12}$$

$$u_2 = \begin{cases} \left|1 - \frac{|B_A(\psi_{min})[\bar{\mathbf{a}}]|}{\omega C_{IC}(N_{max})}\right| \\ \text{if } C_{IC}(N_{min}) \leq -\frac{B_A(\psi_{min})}{\omega} \leq C_{IC}(N_{max}) \\ 1 \qquad \text{otherwise} \end{cases} \tag{13}$$

$$u_3 = \begin{cases} \frac{\max\limits_j [P_{to}(\psi_j)[\bar{\mathbf{a}}]]}{P_{av,max}} & \text{if } \max\limits_j \{P_{to}(\psi_j)[\mathbf{a}]\} \leq P_{av,max} \\ 1 & \text{otherwise} \end{cases} \tag{14}$$

with $B_A(\psi_j)[\bar{\mathbf{a}}]$ indicating the susceptance of a tag antenna, with sizes $\bar{\mathbf{a}}$, with respect to the boundary condition $\psi_j \in [\psi_{min}, \psi_{max}]$. The sub-penalties u_1 and u_2 enforce the mapping of tag susceptance over the useful self-tuning range in (10), while u_3 enforces the minimization of the activation power. Sub-penalty weights are defined to satisfy the condition $\Sigma_m w_m = 1$.

IV. Example of application to a Radiofrequency Finger Augmentation Device (R-FAD)

The above procedure is now demonstrated as an example through the design of a reference loop-coupled meandered tag for application over the fingertip. The interrogating unit is placed onto the wrist so that a near-field coupled reader-tag system is obtained [10]. The link performance (i.e. the transducer power gain, and accordingly the turn-on power) have to be insensitive to the touched objects to achieve, for instance, a robust restoration of tactile temperature feeling in impaired people. In this case, the variable boundary condition parameter is the permittivity of the touched object ($\psi \equiv \varepsilon$). The considered self-tuning RFID IC is the Axzon Magnus-S3 that is also provided with an embedded temperature sensor (not exploited in this paper). Impedance parameters are $N_{min} = 80$, $N_{max} = 420$, $G_{IC} = 0.438\ mS$, $C_{min} = 1.9\ pF$, $C_{step} = 1pF/512$ and power sensitivity $p_{IC} = -16.6\ dBm$. This IC also returns the tuning code n following a standard RFID interrogation command.

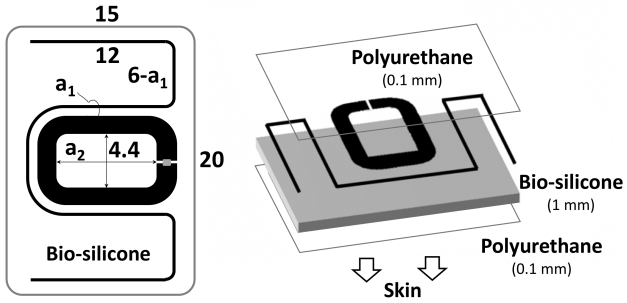

a) b)

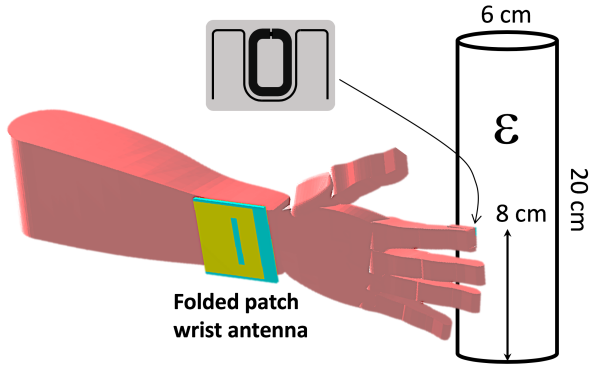

c)

Figure 3. Loop-match dipole used as fingertip tag over a 1 mm thick layer of bio-compatible silicone. a) Tag layout (size in [mm]); b) exploded view of multi-layers for application over the skin. c) The numerical model of the whole R-FAD system. Wrist folded-patch antenna as in [17].

A. Numerical optimization

The fingertip tag to be optimized is a rectangular loop coupled to a meandered dipole covering the area of a typical fingertip (Fig. 3.a). The loop consists of a 35 μm aluminum trace, while the meandered dipole is made by a copper wire having 40 μm radius. The loop is stuck onto the fingertip

This article has been accepted for publication in a future issue of this journal, but has not been fully edited. Content may change prior to final publication. Citation information: DOI 10.1109/TAP.2020.2995315, IEEE Transactions on Antennas and Propagation

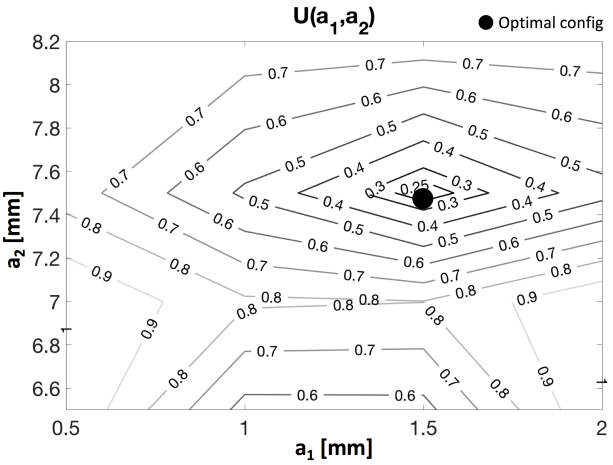

Figure 4. Penalty function U with the indication of the optimal couplet $\{a_1, a_2\}$.

through a 1 mm thick biocompatible silicone layer ($\varepsilon_r = 2.5$, $\sigma = 0.005\ S/m$) that is used as a spacer to reduce the interaction with the lossy human body. The touched object is represented as a cylinder (height 200 mm; radius 30 mm) made of 0.3 mm thick PET ($\varepsilon_r = 2.5$ [15]) filled with air ($\varepsilon_{min} = 1$) or distilled water ($\varepsilon_{max} = 78$, $\sigma_{max} = 0.05\ S/m$ [16]) in order to account for two extreme boundary conditions. The fingertip tag touches the cylinder at a height of 80 mm from the bottom (Fig. 3). The wrist interrogator antenna is the wearable folded-patch antenna in [17]. The maximum input power is limited to $P_{av,max} = 27$ dBm that is a typical value of battery-driven RFID readers which are suitable to be integrated within a wrist module.

Having fixed the external size of the meandered dipole (15 x 20 mm^2) so that the tag can fit the area of a typical fingertip, the selected parameters for the optimization are the distance a_1 between the loop and the wire and the major axis a_2 of the loop (Fig. 3a). $\overline{\mathbf{a}} = \{a_1, a_2\}$ is optimized in the ranges ($0.5\ mm \leq a_1 \leq 2\ mm$), and ($6.5\ mm \leq a_2 \leq 8.2\ mm$) by minimizing the penalty function as in (11; weights: $w_1 = 0.25$, $w_2 = 0.25$, $w_3 = 0.5$). The numerical simulations required to extract the Admittance matrix $[Y(\varepsilon_j)[\overline{\mathbf{a}}]]$ of the entire R-FAD system (Fig. 3) were performed by CST Microwave Studio 2018.

Fig. 4 shows the contour plot of the penalty function. The optimal configuration (smallest *U*) corresponds to the parameters $\overline{\mathbf{a}} = \{a_1 = 1.5\ mm; a_2 = 7.5\ mm\}$. The performance of the optimal R-FAD system, namely the required activation powers and the returned *n* codes for two boundary configurations, are listed in Tab. I. The trade-off imposed by the strict constraints returned a retuning range $|n(\varepsilon_{max}) - n(\varepsilon_{min})| = 182$, meaning that only half of the retuning capability of the IC ($N_2 - N_1$=340) is sufficient to match the power requirement. In both the extreme boundary conditions the estimated requested power to be emitted by the interrogator is lower than 23 dBm.

Fig. 5 shows the simulated power transfer coefficient of the tag for the two dielectric configurations. Thanks to the self-tuning mechanism of the IC, the power transfer coefficient is $\tau > 0.7$ within the ETSI band (865-868 MHz) for both cases of air and water, in spite of their huge dielectric

Table I
NUMERICAL RESULTS: TURN-ON POWER AND SENSOR CODE *n* FOR THE OPTIMAL CONFIGURATION.

Simulated values [870 MHz]	**Air** ($\varepsilon_1 = 1$)	**Water** ($\varepsilon_2 = 78$)
P_{to} [dBm]	19	22.9
n	339	157

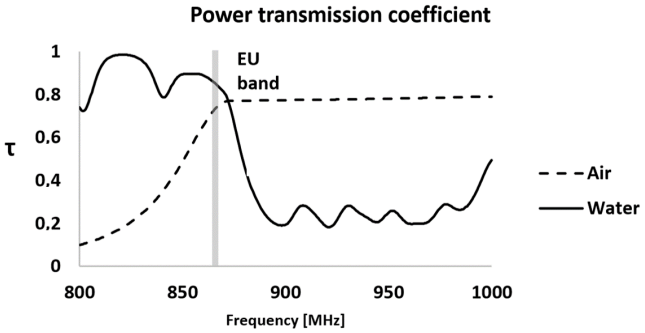

Figure 5. Simulated power transmission coefficient τ of the optimized fingertip tag in reference air condition and when it touches a water-filled bottle. The gray area highlights the target ESTI frequency band of the device

contrast. The small differences between the values of τ while contacting air and water are due to variations in the antenna susceptance (mainly related to the different conductivity of the two materials), which is not compensated by the self-tuning mechanism.

B. Experimental Corroboration

A prototype of the whole R-FAD systems, including the wrist-mounted patch (Fig. 6.b) and the optimized fingertip tag, was experimentally characterized. The ThingMagic M6e

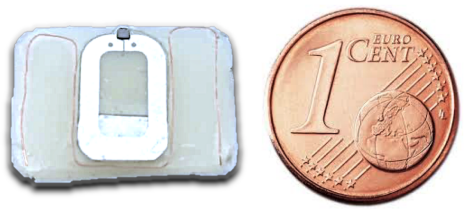

a)

b)

Figure 6. a) Prototype of optimized fingertip antenna; b) entire R-FAD system comprising the fingertip tag applied on the index and a folded-patch antenna integrated within a wristband and connected by a coaxial cable to aThingMagic M6 reader (not visible in the figure) for the measurement of the transducer power gain G_T of the link.

reader was connected to the wrist antenna and driven by a custom test software running on a notebook. The transducer power gain was derived from the measured turn-on power as $G_T = p_{IC}/P_{to}$ for three configurations: fingertip in air, fingertip touching a PET bottle filled with water - as in the previous numerical simulations - plus an intermediate case considering ethyl alcohol ($\varepsilon = 17$, $\sigma = 10^{-5}$ S/m [18]) as filling liquid.

The measured power transducer gains and the tuning code *n* are compared (Fig. 7 and Table II) with simulations involving the two-port model of the self-tuning tag. The ± 3 dB shadowed region around the nominal simulated curves accounts for *i*) the unpredictable variability of users' hand form factor and morphology w.r.t. the oversimplified homogeneous hand model [10], *ii*) the approximated manual deposition of the wire conductor to form the fingertip meandered dipole and *iii*) the real-life fingertip-bottle touch that is far to be sharp (and sweat-free) as in the simulations. Overall, the experimental outcomes reasonably confirm the expected results. It is moreover clear that the measured transducer gain values at 870 MHz are nearly the same ($G_T \cong -39$ dB) for the three considered dielectric boundary conditions. Accordingly, the communication performance of the system can be considered robust and rather insensitive to the variability of the touched object as enforced by the optimization procedure.

Table II
COMPARISON BETWEEN SIMULATED AND MEASURED VALUES AT 870 MHz.

	Air	**Alcohol**	**Water**
ε	1	17	78
***n*, estimated**	339	187	157
***n*, measured**	327 ± 9	185 ± 34	119 ± 24
G_T**, estimated**	$-35,6 \pm 3$ dB	$-35,3 \pm 3$ dB	-39.5 ± 3 dB
G_T**, measured**	-38 ± 1.7 dB	-39 ± 1 dB	-39 ± 1 dB

V. CONCLUSIONS

The presented constrained design method for RFID tags including self-tuning ICs permits to exploit and master the full potentiality of this new family of IC, also in case of complex configurations where the far-field approximation can not be used. The experimental validation with an R-FAD system corroborated the numerical results with a nearly invariant antenna response even when the tag interacts with materials of up to 70 units of dielectric contrast.

The proposed two-port formulation could be moreover used to maximize the IC retuning when the tag is attached to different objects. In this way, the so obtained high-contrast retuning code *n* will provide an indirect indication of the touched material, as preliminary demonstrated in [17], with interesting future applications to sense augmentation, Soft Robotics and Tactile Internet.

ACKNOWLEDGEMENTS

Work funded by Regione Lazio (by the way of Lazio Innova), project Gruppi di Ricerca SECOND SKIN. Ref. 85-2017-14774.

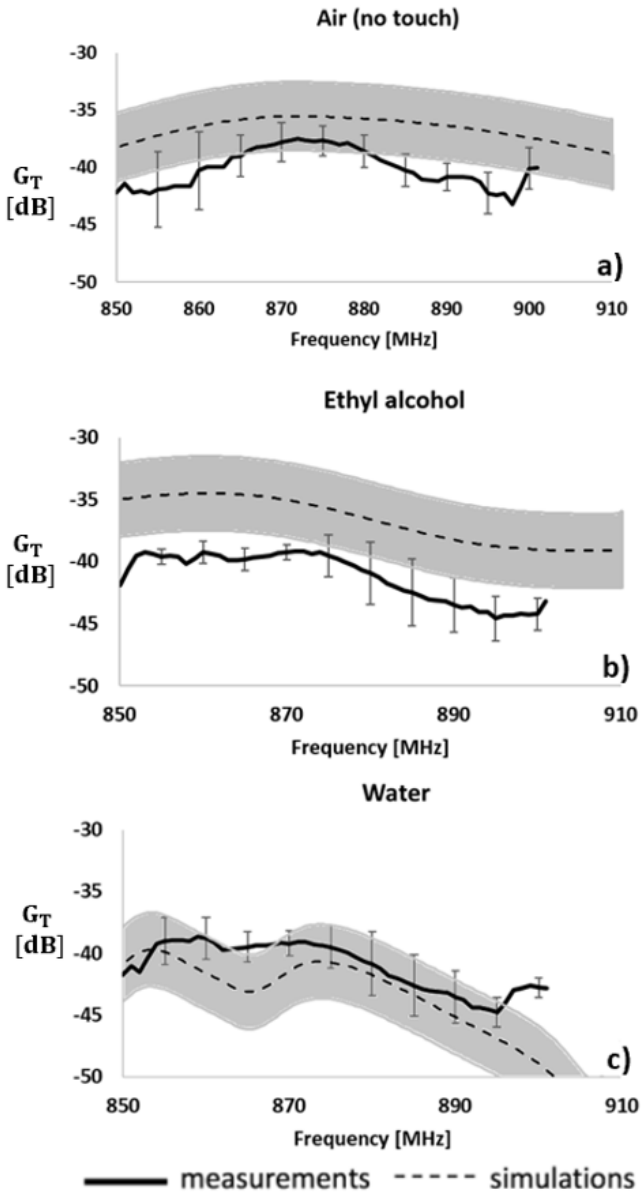

Figure 7. Measured and simulated transducer power gains of the optimized R-FAD for three configurations of the fingertip: a) absence of contact, b) touching a bottle filled with alcohol and c) with water. The ± 3 dB shadowed regions account for the approximation of the hand model w.r.t. real hands, the manufacturing tolerances of the tag and the not perfect adhesion of tag to the finger skin. The standard deviations of the measurements relate to the repetition of measurements with three prototypes for each configuration.

REFERENCES

[1] Magnus™ UHF RFID Tag IC, RFID tag chip antenna design guideline, Application Note [Online]. Available: www.rfmicron.com.

[2] Monza® R6 Tag Chip Datasheet, Application Note [Online]. Available: www.impinj.com.

[3] NXP UCODE 8/8m [Online]. Available: https://www.nxp.com/docs/en/data-sheet/SL3S1205-15-DS.pdf

[4] M. C. Caccami and G. Marrocco, "Electromagnetic Modeling of Self-Tuning RFID Sensor Antennas in Linear and Nonlinear Regimes,", *IEEE Trans. Antennas Propagation*, vol. 66, no. 6, pp. 2779-2787, June 2018.

[5] K. Zannas, H. El Matbouly, Y. Duroc and S. Tedjini, "Self-Tuning RFID Tag: A New Approach for Temperature Sensing," in IEEE Transactions on Microwave Theory and Techniques, vol. 66, no. 12, pp. 5885-5893, Dec. 2018.

[6] C. Miozzi, V. Errico, G. Saggio, E. Gruppioni and G. Marrocco, "UHF RFID-Based EMG for Prosthetic Control: preliminary results," *2019 IEEE International Conference on RFID Technology and Applications (RFID-TA)*, Pisa, Italy, 2019, pp. 310-313.

[7] E. Moradi et al., "Backscattering Neural Tags for Wireless Brain-Machine Interface Systems," in *IEEE Transactions on Antennas and Propagation*, vol. 63, no. 2, pp. 719-726, Feb. 2015.

[8] M. W. A. Khan, L. Sydänheimo, L. Ukkonen and T. Björninen, "Inductively Powered Pressure Sensing System Integrating a Far-Field Data Transmitter for Monitoring of Intracranial Pressure," in *IEEE Sensors Journal,* vol. 17, no. 7, pp. 2191-2197, 1 April1, 2017.

[9] R. Lodato and G. Marrocco, "Close Integration of a UHF-RFID Transponder Into a Limb Prosthesis for Tracking and Sensing," in IEEE Sensors Journal, vol. 16, no. 6, pp. 1806-1813, March15, 2016.

[10] S. Amendola, V. Di Cecco and G. Marrocco, "Numerical and Experimental Characterization of Wrist-Fingers Communication Link for RFID-Based Finger Augmented Devices", *IEEE Transactions on Antennas and Propagation*, vol. 67, no. 1, pp. 531-540, Jan. 2019.

[11] S. Lopez-Soriano, I. P. Spassovsky, J. Parron and G. Marrocco, "Electromagnetic feasibility of a passive wireless sensor network for temperature mapping inside a shielded enclosure," 2017 11th European Conference on Antennas and Propagation (EUCAP), Paris, 2017, pp. 1995-1998.

[12] S. Nappi, N. D'Uva, S. Amendola, C. Occhiuzzi and G. Marrocco, "A near-field RFID sensor network for the realtime monitoring of tire vulcanization," 2017 IEEE International Conference on RFID Technology & Application (RFID-TA), Warsaw, 2017, pp. 69-73.

[13] R. Trevisan and A. Costanzo, "A UHF Near-Field Link for Passive Sensing in Industrial Wireless Power Transfer Systems," in IEEE Transactions on Microwave Theory and Techniques, vol. 64, no. 5, pp. 1634-1643, May 2016.

[14] G. P. Fettweis, "The Tactile Internet: Applications and Challenges," in IEEE Vehicular Technology Magazine, vol. 9, no. 1, pp. 64-70, March 2014

[15] V. Svorˇc´ik, O. Ekrt, V. Rybka, J. Lipta´k, V. Hnatowicz, ''Permittivity of polyethylene and polyethyleneterephtalate", *Journal of Materials Science letters*, 2000, pp. 1843–1845

[16] C. G. Malmberg and A. A. Maryott, "Dielectric Constant of Water from 0 0 to 1000 C", *Journal of Research of the National Bureau of Standards*, 1956

[17] G. M Bianco, G. Marrocco, "Fingertip Self-tuning RFID Antennas for the Discrimination of Dielectric Objects", *13th European Conference on Antennas and Propagation (EuCAP),* Krakow, Poland 2019

[18] R.J. Sengwa, ''Comparative dielectric study of mono, di and trihydric alcohols", *Indian Journal of Pure & Applied Physics*, 2003